Mass Transfer from a Soluble Solid Sphere

F. H. GARNER and R. D. SUCKLING

The University of Birmingham, Birmingham, England

Mass transfer from 3/8- and 1/2-in.-diameter spheres of adipic acid and from 3/8-, 1/2-, 5/8- and 3/4-in.-diameter spheres of benzoic acid into a controlled stream of water passing in laminar flow through a 3-in.-diameter pipe is found to be correlated by the single equation $N_{Sh} = 2 + 0.95\ N_{Re}^{0.5}\ N_{Sc}^{0.33}$ for sphere Reynolds numbers between 100 and 700. The limitations on the application of this equation, due to mass transfer by natural convection, are discussed. Correlations are also obtained for transfer from separate regions of the sphere surface.

Skin-friction-drag coefficients for single fixed spheres have been calculated from reported pressure distributions for Reynolds numbers between 100 and 1,000.

Good agreement is obtained between the mass transfer j factor and other reported values for heat transfer, but comparison with the calculated frictional forces indicates that the equality proposed by Colburn (*3*) does not hold, because the distributions of the mass transfer and the skin friction over the surface differ.

Mass transfer from single spheres to a liquid has received little attention and the analogy between mass and momentum transfer has not been investigated, chiefly because of the lack of data for the values of the skin friction of a sphere.

This work forms part of the more general study of mass transfer processes being undertaken at present in the Chemical Engineering Department of Birmingham University and it was considered that this work would provide data of use for predicting not only mass transfer from solid surface but also for predicting outside film coefficients in liquid-liquid extraction and gas absorption.

The relation between momentum and mass transfer from single spheres with liquid is unknown largely because of lack of knowledge of the skin friction around a sphere and there have been few investigations of the rate of solution at various points around a sphere corresponding to a sphere freely falling or rising in a liquid.

Such knowledge is highly desirable in that a solid sphere is the prototype of an undistorted liquid drop or gas bubble, and it has been shown that the flow conditions around a drop or bubble are precisely analogous to those around a solid sphere (*10*), contrary to some of the supporters of the penetration theory who postulate slip at fluid interfaces.

MOMENTUM TRANSFER

When a real fluid flows over a solid body there is normally no slip between the fluid and the solid surface and there is a velocity gradient outward from the surface, resulting in a net force on the body acting in the direction of the fluid stream, called the *skin friction drag*.

For flow over cylinders or spheres the flow pattern is not symmetrical forward and aft of the body, owing to the dissipation of energy by the internal viscous forces. The pressure difference across the body results in another force, known as *form drag*, acting on the body in the direction of the fluid stream. Summation of these two drag forces gives the total drag force experienced by the body, and these forces are usually expressed in terms of a dimensionless drag coefficient which for a sphere may be written as

$$C_D = \frac{\text{drag force}}{\frac{1}{2}\rho V_0^2 \pi r^2} \qquad (1)$$

For spheres the total drag is usually determined by measurement of the terminal velocity of freely falling spheres, but this gives no indication of the relative importance of skin friction and form drag. The contribution of the frictional drag can be found directly only from an analysis of the hydrodynamic conditions over the sphere surface, usually based upon the variation of the normal pressure over the surface. Values obtained in this way by McNown and Newlin (*20*) indicate that skin friction represents less than 7% of the total drag over the range of Reynolds numbers between 6×10^3 and 2×10^5. For lower Reynolds numbers, Tang, Duncan and Schweyer (*30*) have derived an expression for the estimation of the skin friction, but as it is based upon pressure data determined at a Reynolds number of 16.5×10^4, it is not suitable for Reynolds numbers of 10^3 and below, since the conditions over the surface are very different.

The values obtained for the skin friction in the present work are calculated from pressure distributions determined by Grafton (*12*). These were obtained from a ½-in.-diameter phosphor-bronze sphere mounted in the center of a stream of water flowing through a 3-in.-diameter pipe. The velocity, under streamline flow conditions, was varied from 10^2 and 10^3 Reynolds numbers. The method of analysis used involves the calculation of the hydrodynamic boundary-layer thickness δ, which can be used to determine the intensity of the skin friction over the surface. Graphical integration is then used to obtain the skin-friction drag coefficient.

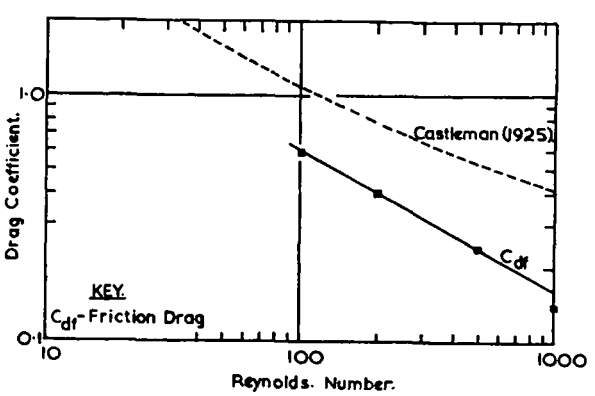

Fig. 1. Amended values for drag coefficients.

Numerous methods of mathematical analysis are available for the surface up to the position of separation of the forward flow. Of these the method of Tomotika (*31*) was used, based on his solution of the momentum integral equation of Milikan (*22*) for a three-

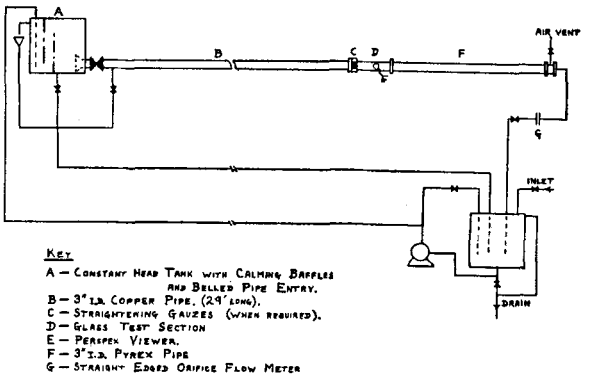

Fig. 2. Diagrammatic arrangement of apparatus.

dimensional boundary layer, the Pohlhausen quartic velocity distribution being assumed within the layer.

The area beyond separation, i.e., the wake region, is less susceptible to mathematical analysis; Grafton (*12*) derived a solution of Milikan's equation by the assumption of a quartic velocity distribution with two further assumptions. Since the pressure measurements in the wake region show little variation, pressure was assumed to be constant over the surface within the wake and, in addition, no discontinuity in the boundary-layer thickness is assumed at separation. With these assumptions Grafton obtained the expression

$$\delta^2 = 34.054\left(\frac{r\nu}{U}\right)\phi(\theta_1) \qquad (2)$$

where $\phi(\theta_1)$ is a trigonometric function of θ_1, the angle measured from the rear stagnation point, and U is the velocity at the outer edge of the boundary layer. Since the value of U in the wake is not known, it is expressed in terms of the circulation velocity in the wake as indicated by red-ink traces of the flow patterns. This circulation velocity is also assumed constant and its value at the actual values of the boundary-layer thickness are found by making the value of δ continuous at the separation point.

The chief disadvantage of this method of solution is the need for a red-ink trace of the flow pattern within the vortex region. The assumptions are also open to the following criticisms: The assumption of constant pressure over the surface implies a constant velocity at the outer edge of the boundary layer but the results show that the velocity alters quite rapidly close to the rear stagnation point and the separation point, although over most of the region it is almost constant; and also observation of the circulation by means of aluminum particles indicates that the velocity is not constant around the vortex, the fluid being accelerated along the outer edge of the wake and retarded near the sphere surface. Despite these limitations, and in the absence of any other method, it is felt that this method gives a useful indication of the conditions within the wake.

The skin-friction-drag coefficients obtained from these calculations are given in Table 1 together with the calculated circulation velocities and the free stream velocity. It will be noted that at Reynolds number 1,000 the circulation velocity is predicted to be twice the main-stream velocity. This is not possible, as the main stream provides the driving force for the vortex by means of viscous forces. At the lower end of the range at $N_{Re} = 82$, Grafton (*12*) observed a circulation velocity equal to one half the main stream velocity and this agrees with the values predicted at Reynolds numbers of 200 and 500. In these two cases the wake skin friction is 8.2 and 7.3%, respectively, of the value for the forward flow area. In the absence of any alternative method of calculation, the skin friction in the wake is assumed to be 7½% of that for the forward flow area for all cases in the region under consideration. The values of the skin-friction-drag coefficients recalculated on this basis are given in Table 2.

The negative values given for the wake are explained by the flow along the surface being in the reverse direction to that of the main stream and so producing a drag in the reverse direction. These amended values and the curve presented by Castleman (*2*) for the total drag coefficient are illustrated in Figure 1.

MASS TRANSFER PROCESSES

At the interface between a soluble solid and a liquid a saturated solution is formed as shown by Ward and Brooks (*32*). Transfer of the solute into the main body of the fluid occurs in three ways, dependent upon the conditions. For an infinitely small sphere in an infinite stagnant fluid, transfer will be by molecular diffusion alone but, as the sphere size increases, natural convection currents are set up owing to the difference in density between the pure solvent and the solution. This induced flow helps to carry solute away from the interface. The third mode of transfer, forced convection, closely resembles natural convection except that the flow pattern is imposed upon the fluid by an external force. In practice, all three modes of transfer are usually present.

The reported values of mass transfer by molecular diffusion alone are usually obtained by extrapolation from results obtained for small spheres under natural convection conditions. Fuchs (*8*) showed theoretically that the limiting value of the dimensionless mass transfer Sherwood number (KD/D_v) is 2.0 when the sphere becomes infinitely small. This limiting value was confirmed by Langmuir (*16*) from a consideration of the experimental results of Morse (*23*) on diffusion from small spheres of iodine in natural convection and by Whytlaw-Gray and Patterson (*33*) for the sublimation of benzophenone spheres in still air.

Under convective conditions, either natural or forced, a relationship for mass transfer similar to the relationships obtained for heat transfer may be expected, of the form

$$N_{Sh} = f(N_{Re}N_{Sc}N_{Gr'}) \qquad (3)$$

where N_{Sh}, N_{Re}, N_{Sc} and $N_{Gr'}$ are respectively the Sherwood, Reynolds, Schmidt, and Grashof numbers for the mass transfer. Such a relationship has been obtained theoretically by Eckert (*6*) from a consideration of the boundary conditions.

For transfer under natural-convection conditions, where the Reynolds number is unimportant, this expression reduces to

$$N_{Sh} = f(N_{Sc}N_{Gr'}) \qquad (4)$$

The data obtained by Ranz and Marshall (*26*) for the evaporation of water drops in still air are correlated by an expression of this form, namely,

$$N_{Sh} = 2.0 + 0.60N_{Gr}^{0.25}N_{Sc}^{0.33} \qquad (5)$$

Most other work, both theoretical and practical, produces results of the form

$$N_{Sh} = \text{constant} \times (N_{Gr'}N_{Sc})^{0.25} \qquad (6)$$

The most reliable form of this seems to be that derived by Merk and Prins (*21*), which for heat transfer from a sphere is written as

$$N_{Nu} = 0.558(N_{Gr'}N_{Pr})^{0.25} \qquad (7)$$

However, this takes no account of the effect of the "plume" of hot air rising above the sphere.

Under forced convection conditions where the Grashof number is unimportant the general expression becomes

$$N_{Sh} = f(N_{Re}N_{Sc}) \qquad (8)$$

which boundary layer theory suggests should take the form

$$N_{Sh} \propto N_{Re}^{0.5}N_{Sc}^{0.33} \qquad (9)$$

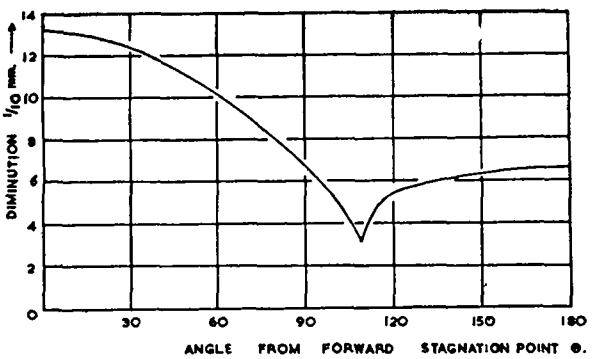

Fig. 3. Distribution of mass transfer.

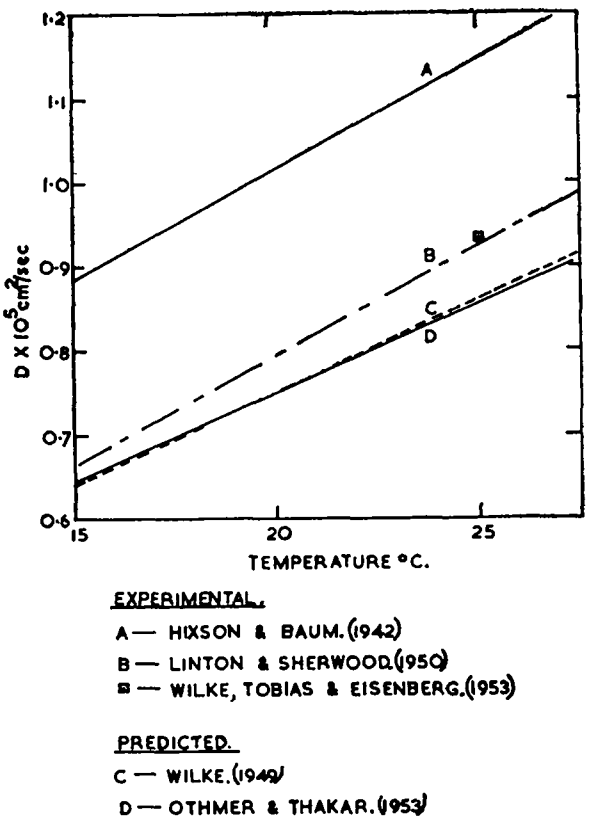

Fig. 4. Diffusivity data for benzoic acid in water.

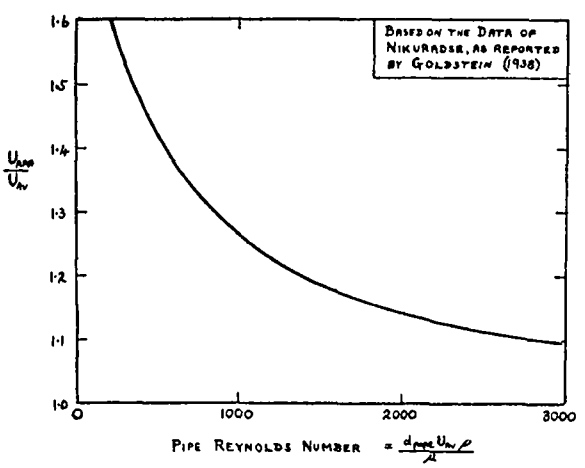

Fig. 5. Velocity at sphere position in distributed flow.

Correlations of this form have been obtained by experiment over quite a wide range of Reynolds numbers; Frössling (*7*) from a study of the mass transfer from liquid spheres of nitrobenzene, aniline, and water and from solid spheres of naphthalene to air for diameters of 0.02 to 0.18 cm. derives a relationship which may be written in the form

$$N_{Sh} = 2.0 + 0.55 N_{Re}^{0.5} N_{Sc}^{0.33} \quad (10)$$

for Reynolds numbers between 2 and 1,000. Similarly at slightly higher Reynolds numbers, 600 to 2,600, Axel'rud (*1*) obtains the expression

$$N_{Sh} = 0.82 N_{Re}^{0.5} N_{Sc}^{0.33} \quad (11)$$

for the dissolution of potassium chloride and potassium nitrate spheres in water by use of dissolution periods of 3 to 4 min.

In the field of heat transfer Kramers (*14*), from a study of heat losses from induction-heated spheres, proposes the slightly different expression

$$N_{Nu} = 2.0 + 1.3 N_{Pr}^{0.15} + 0.66 N_{Re}^{0.5} N_{Pr}^{0.31} \quad (12)$$

for the range $0.5 > N_{Re} > 2{,}000$.

In intermediate regions where neither the Reynolds nor the Grashof number can be neglected no satisfactory relationships have been reported. Dryden, Strang, and Withrow (*5*) note that the mass transfer from a packed bed depends upon the direction of flow, i.e., upward or downward, at low Reynolds numbers, which indicates that the natural- and forced-convection flows are interacting. The results of Kramers and Frössling quoted above suggest that the Grashof number is unimportant above $N_{Re} = 1$, but these results were obtained in air and for small-diameter spheres, which give very small Grashof numbers. The only suggested correlations in this intermediate region are the one due to Ranz and Marshall (*26*), who propose a vectorial addition of the velocities, using a natural-convection velocity based upon a modified Grashof number, and the suggestion of Garner and Grafton (*9*) that the transfers due to the two processes are simply additive.

Variation of the transfer rate around the sphere has not been widely studied. Distributions are reported by Frössling (*7*) and by Garner and Grafton (*9*), but the importance of the wake area in mass transfer is not widely known.

EXPERIMENTAL PROCEDURE

The apparatus, shown diagrammatically in Fig. 2, consists essentially of a 3-in. I.D. horizontal water tunnel fitted with reservoir tanks and a recirculation system. A 30-gal. reservoir fitted with calming baffles discharges through a belled entry into a 29-ft. length of 3-in. I.D. straight copper pipe. This is followed by a 1-ft. working section of 3-in. I.D. glass pipe and a further 5-ft.

TABLE 1

CALCULATED CIRCULATION VELOCITIES AND DRAG COEFFICIENTS

Reynolds Number	100	200	500	1,000
Free stream velocity, cm./sec.	0.811	1.62	4.05	8.11
Wake velocity, cm./sec.	0.063	0.90	2.05	16.0
Ratio, wake: stream	0.077	0.55	0.51	1.97
Skin-friction-drag coefficients				
Front	0.640	0.438	0.260	0.155
Wake	−0.001	−0.036	−0.019	−0.145
Total	0.64	0.40	0.24	0.01

TABLE 2

AMENDED VALUES OF SKIN-FRICTION-DRAG COEFFICIENT

Reynolds number	100	200	500	1,000
Skin-friction-drag coefficient				
Front	0.640	0.438	0.260	0.155
Wake	−0.048	−0.033	−0.020	−0.012
Total	0.59	0.40	0.24	0.14

section of glass pipe. The water then flows through a square-edged orifice meter into a tank, from which it is pumped back to the reservoir. Three interchangeable orifice plates are used in the flow meter, which operates a carbon tetrachloride U-tube manometer. With this system the average velocity in the 3-in. pipe can be measured over the range of 0.006 to 0.15 ft./sec.

The belled entry and long length of pipe (approximately 120 diameters) ensure a typical parabolic flow distribution with a minimum of disturbance in the working section. A pack of six 30/30 mesh 33 S.W.G. phosphor-bronze-gauze flow distributors can be placed when required at the end of the copper section to give a flatter velocity front. The actual velocity profile at the sphere position, two pipe diameters downstream from the gauzes, then depends upon the water flow rate, varying from near parabolic at very low flows to nearly flat at high flows.

The spheres of benzoic and adipic acids used in this work were prepared by compressing the acid into pellets in a hand press. This gave pellets having a smooth surface, with no definite crystalline arrangement such as casting would produce. Uniformly high pellet densities of 1.29 to 1.30 g./cc. for benzoic acid and 1.33 to 1.34 g./cc. for adipic acid were obtained by this method. The sphere sizes were $\frac{3}{8}$, $\frac{1}{2}$, $\frac{5}{8}$, and $\frac{3}{4}$-in.-diameter in benzoic acid and $\frac{3}{8}$ and $\frac{1}{2}$ in. in adipic acid.

All the spheres were supported from downstream on a 5-in.-long $\frac{1}{16}$-in.-diameter brass rod, mounted on a $\frac{1}{8}$ by $\frac{1}{32}$-in. brass strip forming a diameter of the 3-in. I.D. test line. The end of the rod was thinned to fit into a 0.046-in.-diam. hole drilled along a radius of the pellet. The supporting rod was fixed so as to be coaxial with the test line.

Dissolution of the spheres was followed photographically with a Bolex 16-mm. ciné camera and back lighting. Single exposures were made at the beginning and end of the dissolution period. The film was projected by means of a Kodascope projector, and drawings of the silhouettes were made approximately twelve times the actual sphere size. In order to reduce the optical distortion caused by the cylindrical pipe wall, a perspex block was cut with one face curved to fit against the pipe wall and the opposite face plane. Cross wires attached to this block served to locate the final photograph with respect to the initial one. The refractive index of the perspex was slightly greater than that of the water in the pipe line, and so a correction factor for the slight optical distortion was calculated in each specific case by comparing the apparent dimensions of equal actual lengths in the natural and distorted planes. The diminution was then measured at 10-deg. intervals around the circumference of the corrected silhouettes.

RESULTS

A typical distribution of the transfer around the surface is shown in Figure 3. The transfer rates for the total surface, the forward flow area (i.e., the area upstream of separation), and the wake area are found from these distributions by graphical integration over the surface, the rates for the forward and rear stagnation points from the terminal values of these curves, and the rates expressed in terms of the Sherwood number.

In order to express the results in terms of the Schmidt and Sherwood numbers, it is necessary to find values for the diffusivity of the materials used. A survey of the literature revealed no experimental data for adipic acid and, since it is difficult to determine the diffusivity experimentally with any degree of accuracy, it was evaluated by the prediction method of Othmer and Thakar (*24*). In order to make the results for adipic and benzoic acids comparable the diffusivity of the latter material was determined in the same way. The agreement between the predicted and experimental values for benzoic acid is good, as shown in Figure 4, where the values predicted by the methods of Othmer and Thakar (*24*) and Wilke (*34*) are compared with the experimental data reported by Linton and Sherwood (*17*) and Hixson and Baum (*13*), and an isolated value quoted by Wilke, Tobias, and Eisenberg (*35*). The values reported by Hixson and Baum were used by Garner and Grafton (*9*) in calculating the results for the dissolution of $\frac{1}{2}$-in.-diameter benzoic acid spheres; as there is a wide discrepancy between these values of the diffusivity and the predicted values, the results of Garner and Grafton have been recalculated by means of predicted values before being combined with the results obtained in the present work.

Since a range of velocity profiles has been used in this work the choice of the velocity used in the Reynolds number is important. The first choice was the velocity at the sphere position, i.e., the approach velocity. This was taken as the average velocity over the cross-sectional area of the sphere and for parabolic flow varied between 1.94 and 1.97 times the average stream velocity, depending upon the size of the sphere. When the gauzes were in position the approach velocity was determined from the correlations of Nikuradse for the development of a parabolic front from uniform distributed flow. The variation of the mean velocity at the sphere position with pipe Reynolds number based upon the average fluid velocity is shown graphically in Figure 5.

By means of the approach velocity the results for the forward stagnation point are shown in Figure 6. Two distinct lines were obtained, one for the parabolic velocity front and the other for the distributed flow. It was then decided to use the average fluid velocity as the basis of the Reynolds number, and this produces quite satisfactory agreement between the two sets of data as shown in Figure 10. The average fluid velocity was therefore used for all the mass transfer correlations.

The experimental results and the calculated values of the film coefficient and the Sherwood number for $\frac{5}{8}$-in.-diameter benzoic acid spheres are given in Tables 3 and 4, being typical of the results obtained.* Figures 7 to 11 show the results obtained for the over-all transfer and the transfer from the forward flow region, the wake region, the forward stagnation point, and the rear stagnation point respectively. The following expressions are proposed to correlate these results.

Over-all transfer

$$N_{Sh} = 2 + 0.95 N_{Re}^{0.5} N_{Sc}^{0.33} \qquad (13)$$

Forward flow area transfer

$$N_{Sh} = 2 + 1.08 N_{Re}^{0.5} N_{Sc}^{0.33} \qquad (14)$$

Wake area transfer

$$N_{Sh} = 2 + 0.67 N_{Re}^{0.5} N_{Sc}^{0.33} \qquad (15)$$

Forward stagnation point

$$N_{Sh} = 2 + 1.68 N_{Re}^{0.5} N_{Sc}^{0.33} \qquad (16)$$

Rear stagnation point

$$N_{Sh} = 2 + 0.87 N_{Re}^{0.5} N_{Sc}^{0.33} \qquad (17)$$

All for the range $100 < N_{Re}^{0.5} N_{Sc}^{0.33} > 300$

Considerable scatter is apparent in the results shown, even for the over-all transfer. This is thought to be introduced in the measurement of the diminution from the projected silhouettes. Even though the

*Tabular material has been deposited as document 5494 with the American Documentation Institute, Photoduplication Service, Library of Congress, Washington 25, D. C., and may be obtained for $1.25 for photoprints or 35-mm. microfilm.

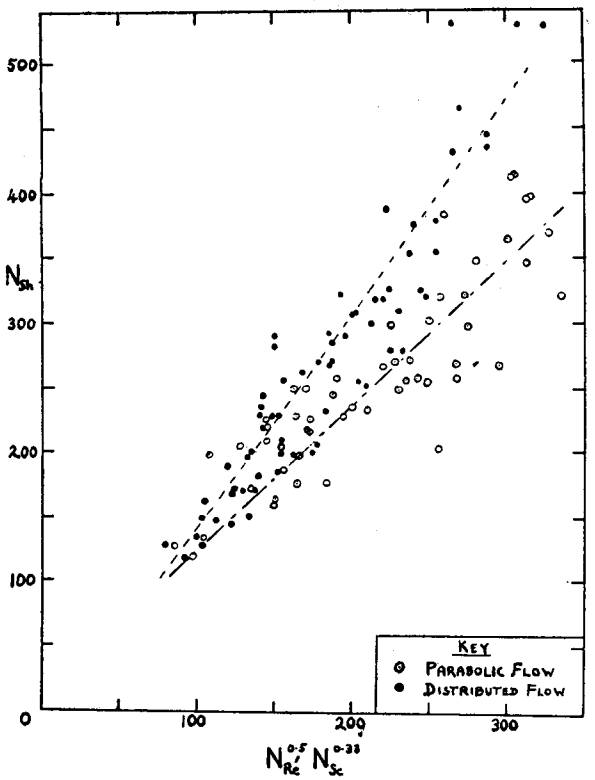

Fig. 6. Mass transfer from forward stagnation point (based on approach velocity).

projected images were approximately twelve times life size the average diminution to be measured was about 6 mm.; thus small errors in measuring either the initial or final silhouette are greatly magnified when the difference is taken. Greater dissolution is not permissible, as it would result in an appreciable change in the Reynolds number and so alter the conditions around the sphere; this change in conditions may account for some of the scatter observed at present. Ideally, the dissolution should be kept as small as possible and the magnification made much greater than that used herein.

The values reported for the separate regions of the sphere also scatter for the same reason and from an additional cause. Accurate measurement is dependent upon the final silhouette being located accurately with respect to the initial one. This was done as carefully as possible by means of the cross wires in the optical system, but again small errors here become large percentages of the actual diminution. Despite this scatter the lines are quite well defined and there is no apparent distinction between different sphere diameters, materials, or velocity profiles.

DISCUSSION OF RESULTS

The general variation of mass transfer rate over the surface of a solid sphere in a controlled stream of water is well defined and is clearly indicated by the results obtained from these dissolutions as illustrated in Figure 3. The exact form of the variation depends upon the Reynolds number of the flow, but over the range studied the example shown is typical. At lower Reynolds numbers the results of Frössling (*7*) indicate that the distribution becomes more uniform.

In general terms this distribution may be explained by means of the boundary-layer concept on the assumption that the mass transfer and hydrodynamic boundary-layer thicknesses are in a constant ratio under a given set of conditions. Progressing from the forward stagnation point around the sphere, the boundary-layer thickness increases and, as the concentration difference across the layer is constant, the concentration gradient will become less steep, thus reducing the point value of the mass transfer rate. A similar process will occur over the surface in the wake commencing at the rear stagnation point. Since the fluid within the wake is continually circulating and is not discharged into the main body of the fluid until the flow attains very high Reynolds numbers, the solute must diffuse from the outer boundary of the vortex region into the bulk of the fluid, and a relatively dilute solution is returned to the rear stagnation point. If this were not the case, the concentration in the wake would build up and the rate of mass transfer from this region would become much lower than that observed. The importance of the wake is therefore due to the large extra surface made available for transfer and to the vortex motion supplying a stream of relatively solute-free solvent to the rear stagnation point.

It will be seen from Figure 3 that there is a pronounced minimum in the mass transfer distribution over the surface. The effect of Reynolds number upon the position of this minimum is shown in Figure 12 together with the curve reported by Garner and Grafton (*9*) for the movement of the hydrodynamic separation point. The values of the Reynolds number are based upon the approach velocity, as defined earlier.

The sphere is a three-dimensional axisymmetrical body and this region of minimum transfer appears as a ring around the surface in the rear half of the sphere, but since all the mass transfer observations have been made from silhouettes the minimum transfer region is seen as two points, one near the top and the other near the bottom of the circle. Throughout this discussion therefore it is referred to as the *point of minimum transfer*. Similarly in the hydrodynamic case a ring of separation is formed at the back of the sphere, but for the purposes of this discussion this also is referred to as a point.

From simple theory it would appear that the separation point and the point of minimum mass transfer should coincide since the hydrodynamic boundary layer attains its maximum thickness at the separation point. This coincidence is observed over the central portion of the curves (Figure 12), but there is distinct separation at either end. At Reynolds numbers above 400 the minimum mass transfer occurs a few degrees behind the separation point. This appears to be due to the presence of a small region of near-stagnant fluid, immediately behind the separation point, in which transfer occurs only very slowly. As the separation point moves further back over the surface with decrease in Reynolds number the angle between the surface and the separating stream line becomes greater and there is less tendency for this stagnant pocket to be formed. The minimum transfer point is also seen to be after the observed position of separation at low Reynolds numbers. In this region, however, natural-convection currents are becoming important and these may induce conditions over the surface which correspond to a different Reynolds number from that of the main fluid stream. Observations by Keey (*15*) on mass transfer from spheres by natural convection indicate the presence of a ring of minimum mass transfer, similar to that obtained in this work, in the region of 150 deg. from the top of the sphere. This corresponds to the state of zero flow in the hydrodynamic case and the "separation point" should be at 180 deg.

For the mass transfer work in general the Schmidt number varies from about 1,100 to 2,200, and, with the Reynolds number based on the average velocity, the range covered lies between 60 and 660; the two materials used show a

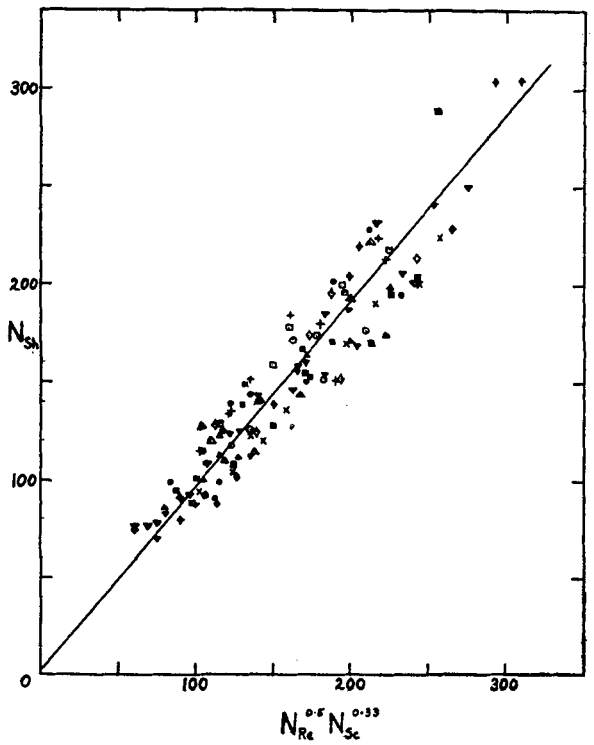

Fig. 7. Over-all mass transfer.

Sphere	Parabolic Flow	Distributed Flow
Benzoic Acid		
3/8" diam	△	▲
1/2" diam	□	■
5/8" diam	▽	▼
3/4" diam	◇	◆
Adipic Acid		
3/8" diam	⊙	●
1/2" diam	×	+

Key to Figures 7 to 15.

distinct difference in solubility, adipic acid being about five times as soluble as benzoic acid, and so it seems that the expression obtained for the over-all transfer:

$$N_{Sh} = 2 + 0.95 N_{Re}^{0.5} N_{Sc}^{0.33}$$

is of general application for values of the group $N_{Re}^{0.5} N_{Sc}^{0.33}$ between 100 and 300 and for sphere diameters not greater than 3/4 in. The inclusion of the constant term satisfies the condition derived by Fuchs (*8*) for transfer by purely molecular diffusion, but no term is included to allow for the natural-convection effects since these appear to be negligible over this range.

This independence of sphere diameter is confirmed by the work of Kramers (*14*) and Tang, Duncan, and Schweyer (*30*) on heat transfer and of Powell (*25*) and Frössling (*7*) on mass transfer. The value of the forced-convection term is in good agreement with that predicted by Grafton (*12*) from the hydrodynamic measurements used earlier in the evaluation of the drag coefficient. This agreement holds not only for the over-all transfer but also for the transfer from the individual parts of the sphere.

At values of the group $N_{Re}^{0.5} N_{Sc}^{0.33}$ less than 100 it is thought that natural-convection effects are becoming important. This is illustrated by the direction of the axis of apparent flow, which is defined as normal to the plane of minimum mass transfer and would, if there were no disturbing forces, lie along the axis of the fluid stream, i.e., along the pipe axis. In practice its position varies with Reynolds number as shown in Figure 13 for 5/8-in.-diameter benzoic acid spheres. At zero Reynolds number mass would be transferred by natural convection only and the axis of apparent flow would be vertical, i.e., at 90 deg. to the pipe axis; as the Reynolds number is increased from zero the two flows interact to produce a net flow directed somewhere between the two individual components. The actual values given in Figure 13 are only approximate since the experimental method was not designed for measurements of this nature, but the effect of increasing Reynolds number can be clearly seen. Above $Re > 100$ the effect of the natural-convection currents is relatively small and the direction of the apparent flow axis becomes constant, presumably along the pipe axis. This result is in line with the deviation noted in the lower Reynolds-number range of the separation-point curve. As a result of this rotation of the flow axis, the forward stagnation point, which in the mass transfer work is taken as the point of maximum transfer, does not coincide with the one defined from hydrodynamic considerations except for Reynolds numbers greater than 200.

Relatively little mass transfer data are available at Reynolds numbers below 60 and no precise relationship can be derived, but an indication of the behavior can be obtained as follows. If it be assumed that the expression derived by Merk and Prins (*21*) for heat transfer from spheres by natural convection, viz.,

$$N_{Nu} = 0.558(N_{Gr} N_{Pr})^{0.25} \qquad (7)$$

has a parallel in mass transfer, then the expression

$$N_{Sh} = 0.60(N_{Gr'} N_{Sc})^{0.25} \qquad (18)$$

may be obtained by making a small addition for the effect of the "tail," which is neglected by Merk and Prins. Assuming a temperature of 20°C. and taking

$$N_{Gr'} = \frac{g D^3}{\nu^2} \frac{\Delta\rho}{\rho}$$

and

$$N_{Sc} = \frac{\nu}{D_v},$$

one obtains the values listed in Table 5.

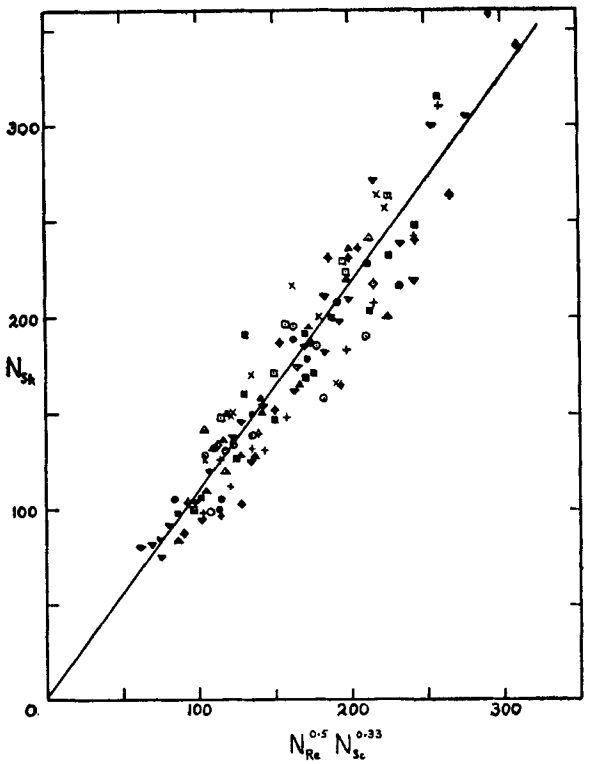

Fig. 8. Mass transfer from forward flow area. See key on Figure 7.

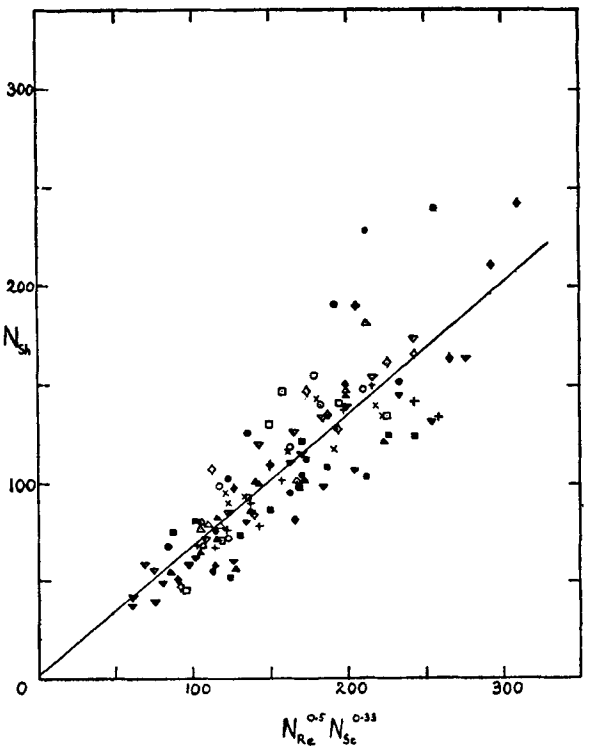

Fig. 9. Mass transfer from wake area. See key on Figure 7.

The Grashof numbers are based upon solution densities determined in this department by Keey (*15*). The transfer at zero Reynolds number can then be described by the expression

$$N_{Sh} = 2.0 + 0.60(N_{Gr'}N_{Sc})^{0.25} \quad (19)$$

which includes the term for the transfer by molecular diffusion. This shows that under these conditions the mass transfer depends upon the sphere size, but in the present study of forced convection the results for all sphere sizes fall on a common line for Reynolds numbers greater than 100 (corresponding to values greater than 110 for the group $N_{Re}^{0.5}$, $N_{Sc}^{0.33}$). So it is suggested that a series of curves exists below this value, where each curve represents the interaction between forced- and natural-convection forces for a given-sized sphere when the forces act perpendicularly, as in this work. If larger diameter spheres were used, the Grashof numbers for the natural-convection transfer would be larger and so presumably the effect would extend to higher Reynolds numbers; thus the correlation obtained in this work is limited to values of $N_{Gr'}$, $N_{Sc} = 1.3 \times 10^8$.

This series of curves could then satisfy the theoretical requirement of Fuchs (*8*) that

$$\left(\frac{dN_{Sh}}{dN_{Re}}\right)_{N_{Re}=0} = 0$$

which is not satisfied by the general correlation proposed for high Reynolds numbers or by many of the previously reported correlations.

The apparatus used in the present work is not suitable to verify the existence of these curves, partly because of the difficulty of flow control and partly because any greater rotation of the flow axis than that experienced at present would require a complex correction for the optical distortion. To facilitate further study in this region a low-speed, vertical water tunnel is under construction; the vertical flow direction will eliminate the rotation of the flow axis due to natural-convection effects and so simplify observations.

The relative importance of the wake in mass transfer is clearly shown in Figure 14. At the lower end of the range, at $N_{Re} = 70$, the wake contributes about 8% of the total transfer; whereas above $N_{Re} \simeq 500$ the curve flattens out, with the wake contributing about 25% of the total. In the range studied there is no indication that the two halves of the sphere will become equally important as observed for cylinders at Reynolds number, 40,000 by Lohrisch (*18*).

The ratio of the mass transferred from the two areas may be written as

$$\text{ratio} = \frac{\text{mass transferred from forward flow area/sec.}}{\text{mass transferred from wake area/sec.}}$$

$$= \frac{2 + 1.08N_{Re}^{0.5}N_{Sc}^{0.33}}{2 + 0.67N_{Re}^{0.5}N_{Sc}^{0.33}} \frac{A_F}{A_W} \quad (20)$$

where A_F and A_W represent the surface areas covered by the forward flow and the wake respectively. Over the range to which these mass transfer relationships apply the values of the second terms are much greater than the constant term, which may therefore be neglected and the expression for the ratio reduced to

$$\text{ratio} = 1.6 \frac{A_F}{A_W} \quad (21)$$

This simple expression suggests that the wake transfer is independent of the size of the vortex region since the outer surface of this grows in extent with Reynolds number faster than the sphere surface included within the wake increases; thus the controlling factor in the total transfer from the wake region

TABLE 5

VALUES OF GRASHOF AND SCHMIDT NUMBERS FOR VARIOUS SPHERES

Spheres, diameter, in.	$N_{Gr'}$	N_{Sc}	0.60 $(N_{Gr'}N_{Sc})^{0.25}$
Benzoic acid			
3/8	3,360	1,340	27.7
1/2	7,970	1,340	34.3
5/8	15,550	1,340	40.6
3/4	26,880	1,340	46.5
Adipic acid			
3/8	34,250	1,525	51.0
1/2	81,200	1,525	63.3

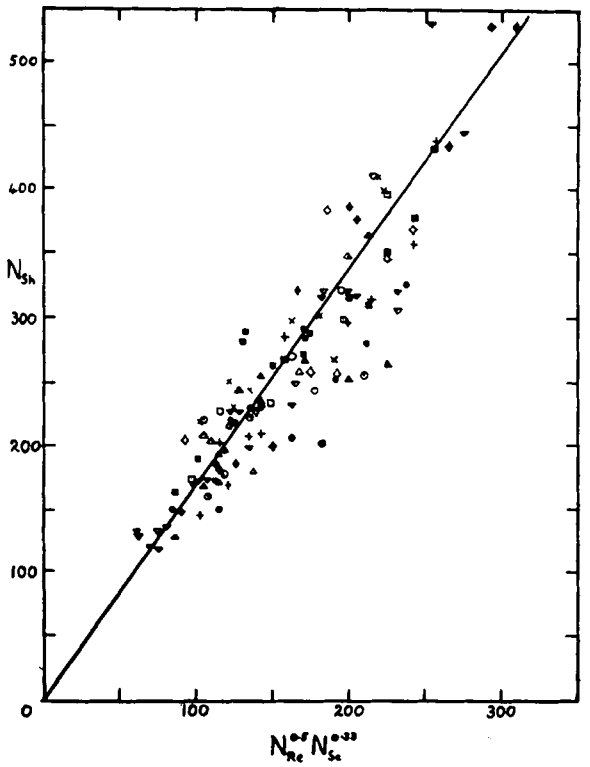

Fig. 10. Mass transfer from forward stagnation point. See key on Figure 7.

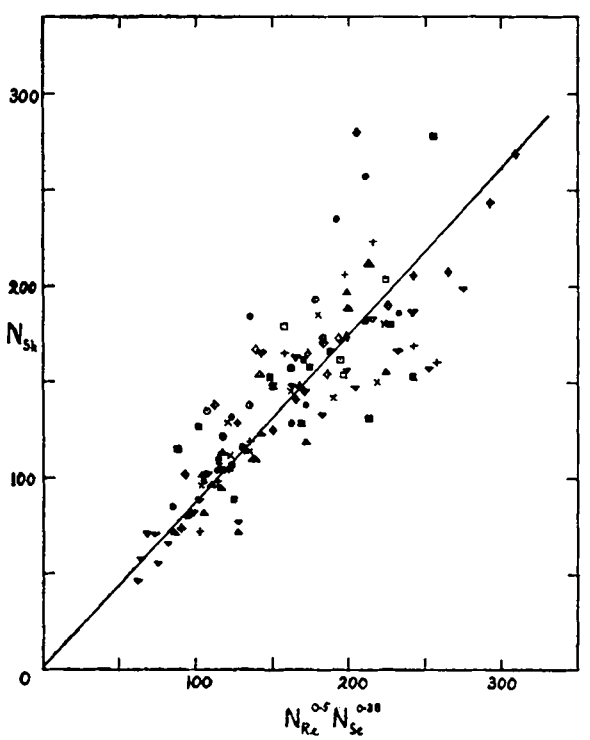

Fig. 11. Mass transfer from rear stagnation point. See key on Figure 7.

appears to be the area of solid surface included within the wake region rather than the extent of the interface available for transfer of solute from the circulating fluid within the wake to the main bulk of fluid.

Thus, over the region to which the mass transfer correlations apply, the mass transfer ratio is determined by the ratio of the areas, which in turn is determined by the position of the separation point. The curve obtained in Figure 14 is, therefore, similar to that obtained for the movement of the separation point, and the results are best correlated by the use of the approach velocity.

It appears then that the position of the separation point and the relative importance of the wake are dependent upon the conditions over the surface as defined by the approach velocity of the fluid, whereas the actual rate of solute transfer is determined by the total mass of fluid flowing. This suggests that there may be a difference between the two processes of mass and momentum transfer for the case of a sphere.

Over most of the region considered above the wakes are of the stable, circulating variety but at Reynolds numbers above 500, periodic oscillations occur at the back of the wake, according to observations reported (*9*) and these might be expected to increase the transfer from the wake. No such effect is noted in this work, but since the highest Reynolds number attained is 660 and the scatter of the data obtained for the wake is quite wide such an effect is not excluded.

ANALOGY BETWEEN MASS AND MOMENTUM TRANSFER

The idea of an analogy between heat, mass, and momentum was first proposed by Reynolds, in the form

$$\frac{K}{G_M} = \frac{h}{C_P G} = \frac{f}{2} \qquad (22)$$

where G is the mass velocity of the fluid
G_M is the molal mass velocity
and $f/2$ is the friction factor

This simple analogy applies under only very limited conditions, mainly for transfer in gases in turbulent flow. The j-factor theory proposed by Colburn (*3*) is a modified form of the original and attempts to allow for the effect of the laminar-flow region over the surface of the body. This is done by introducing the Prandtl and Schmidt numbers to produce the following empirical relationships:

$$\frac{K}{G_M}(N_{Sc})^{2/3} = j_D$$

$$= \frac{h}{C_P G}(N_{Pr})^{2/3} = j_H = \frac{f}{2} \qquad (23)$$

In this form the analogy appears to be of rather wider application although still intended primarily for turbulent-flow conditions.

The term $f/2$ is a measure of the resistance to the fluid motion and for flow in pipes is the Fanning factor. For spheres, however, only that portion of the drag due to skin friction is used since form drag is produced by the pressure difference across the sphere, which has no analogue in the other transfer processes. Moreover, it has recently been suggested by Tang, Duncan, and Schweyer (*30*) that the quantity used should be the total frictional force on the sphere surface and not the skin-friction-drag coefficient. This seems very probable since the drag coefficient contains only the component of the frictional force in the direction of flow and thus requires that the drag in the wake be subtracted from that for the forward flow area; whereas for heat and mass transfer the total transfer from the whole surface is taken, regardless of direction.

The mass transfer data obtained for the over-all transfer in the present work have been expressed in terms of the j factor and are plotted against Reynolds number based on the average velocity in Figure 15. For Reynolds numbers greater than 100 a straight line of slope -0.5 is obtained. This is in agreement with the dependence of the Sherwood number on the square root of the Reynolds number shown in Figure 7, since the j factor can be rewritten for dilute solutions as follows:

$$j_D = \frac{K}{U}(N_{Sc})^{2/3} = N_{Sh}N_{Re}^{-1}N_{Sc}^{-1/3} \tag{24}$$

Then from Figure 15

$$j_D \propto N_{Re}^{-1/2} \tag{25}$$

$$\therefore N_{Sh} \propto N_{Re}^{1/2}N_{Sc}^{1/3} \tag{26}$$

Since the j-factor theory is derived primarily for turbulent conditions no allowance is made for the effect of transfer by natural convection and so at low flow rates the transfer predicted by the relation

$$j_D = \text{constant} \times N_{Re}^{-0.5}$$

is lower than that which actually occurs. This is shown clearly in Figure 15, where the line curves upward at Reynolds numbers below 100. This also agrees with the earlier finding that natural convection becomes important in this region (Figure 13). Even in Figure 15, however, the data are too few and scattered to permit the dependence upon sphere size in this region to be determined properly.

Comparison among the three transfer processes is made in the following table and shown graphically in Figure 16.

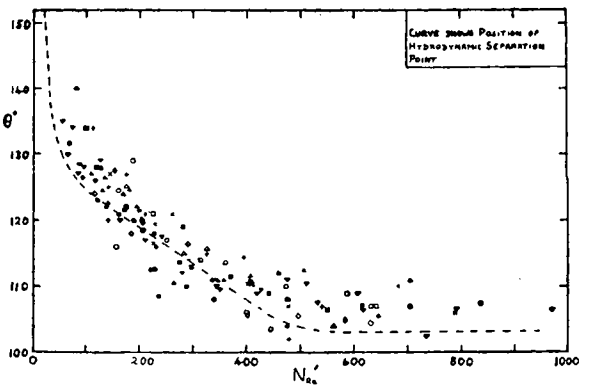

Fig. 12. Variation of position of minimum mass transfer. See key on Figure 7.

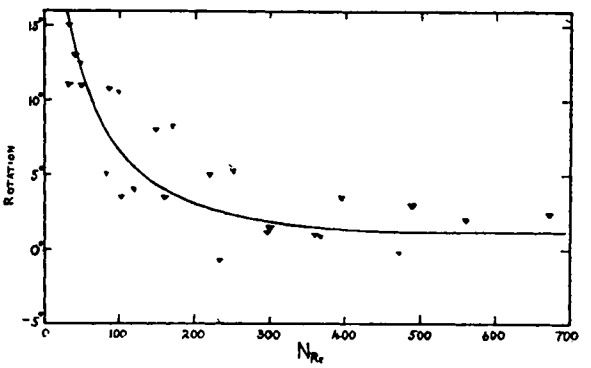

Fig. 13. Augular rotation of apparent flow axis. See key on Figure 7.

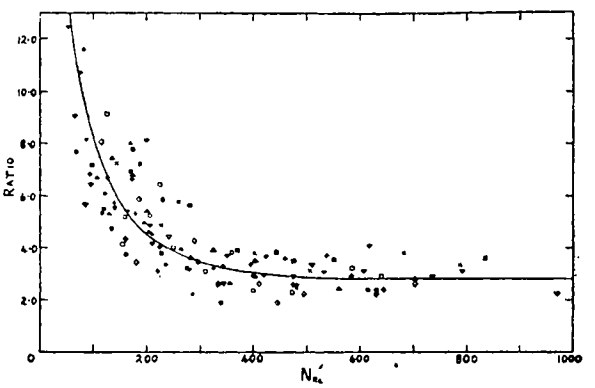

Fig. 14. Ratio of mass transfer (front: wake). See key on Figure 7.

TABLE 6

COMPARISON OF HEAT, MASS, AND MOMENTUM TRANSFER FOR SPHERES

Reynolds No.	100	200	500	1,000
j_D	0.095	0.067	0.042	0.029
j_H	0.102	0.074	0.049	0.035
$C_f/2$	0.104	0.072	0.044	0.025

The mass transfer line is that obtained in this work; that for heat transfer is as quoted by Sherwood and Pigford (*28*) and is a rearranged form of the line recommended for single spheres by McAdams (*19*); and the momentum transfer values are calculated from the skin-friction data presented earlier by means of the total frictional force and the total surface area instead of the component in the direction of flow and the sphere cross-sectional area, as in the drag-coefficient evaluation. The wake now contributes 12% of the forward flow area value compared with 7½% for the drag coefficient and a contribution ranging from 8 to 30% for the mass transfer.

Within experimental error the agreement among the three terms appears quite good and this suggests that the analogy among the transfer processes is applicable to spheres in this Reynolds-number region, when the total frictional force is used as the analogous momentum transfer quantity.

This difficulty in the selection of the analogous drag force does not arise for flow along flat plates or through pipes since form drag is absent and the frictional forces always act in the direction of flow, so that it is not necessary to consider separate components. In these cases the problem is simplified further by the absence of a wake. Thus there seems no reason why the analogy should not apply in these cases, and most experimental evidence suggests that it does. However, as a result of a study of wetted-wall columns, Stirba and Hurt (*29*) suggest that the analogy may apply only under very strictly controlled conditions. They propose that since mass is transferred by the movement of specific molecules rather than by collisions and is the slowest of the three transfer processes, it is the most susceptible to slight degrees of turbulence. This explanation is advanced to account for extremely high mass transfer rates observed in wetted-wall columns under conditions which by all hydrodynamic criteria were laminar, and it is suggested that similar slight unnoticed turbulence may exist in other mass transfer processes. By this theory the mass transfer should be greater than the term used to represent the frictional forces, and the increased transfer may be a phenomenon confined to wetted-wall columns and where there is a pseudostreamline flow at liquid interfaces.

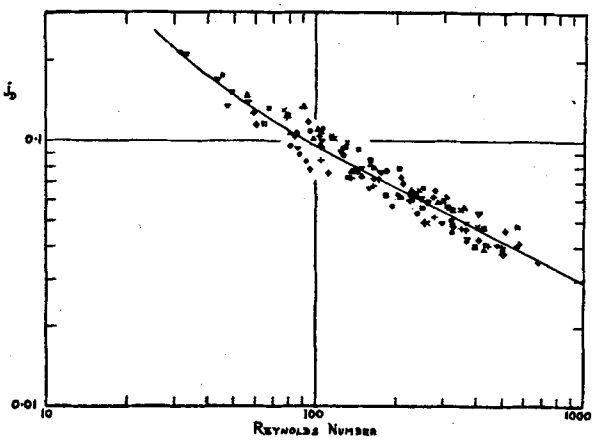

Fig. 15. Mass transfer j factor values. See key on Figure 7.

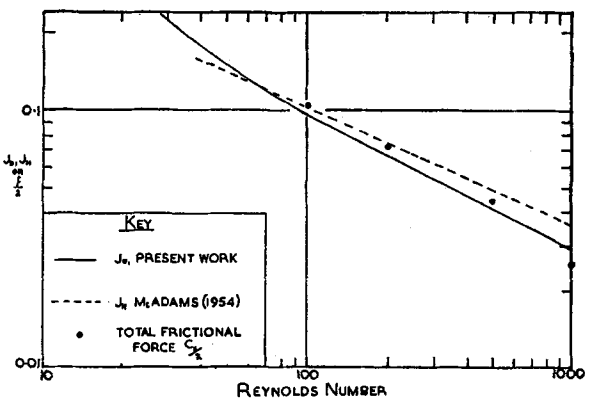

Fig. 16. Comparison of heat, mass, and momentum transfer for spheres.

Considering flow past solid bodies Sherwood (*27*) reports close agreement between the j factors for heat and mass transfer and the skin-friction-drag coefficients given by Goldstein (*11*) for cylinders at Reynolds numbers between 400 and 10,000. If, however, it is accepted that the frictional quantity most nearly analogous to the heat and mass transfer is the total frictional force as used above and not the drag coefficient, the agreement is found to be not nearly so good. From the values given earlier it will be seen that for spheres the total frictional force is about 50% greater than the corresponding value of the drag coefficient and that there must be a corresponding distinction in the case of cylinders, although possibly not so great. Thus if the drag-coefficient values and the j factors are in close agreement, the total frictional force values and the j factors cannot be and the accuracy of the analogy becomes open to question.

It also appears that the good agreement obtained for spheres in the present work may be fortuitous, for in momentum transfer a constant addition of 12% of the forward flow value has been made to allow for the effect of the wake whereas the mass transfer results indicate that the transfer from the wake varies from 8 to 30% of the forward flow value (Figure 14). If the analogy is strictly correct, the contributions of the two portions of the surface should be in the same ratio for both transfer processes, and the distributions of skin friction and mass transfer over the surface should be the same. A typical skin-friction distribution is shown in Figure 17. Comparison of this with the mass transfer distribution (Figure 3) indicates considerable dissimilarity over the forward region of the surface. This again indicates that the analogy does not apply.

CONCLUSIONS

These remarks may be summarized as follows: at low Reynolds numbers some material is transferred by the process of natural convection which has no counterpart in the transfer of momentum and so the complete analogy cannot apply; at higher Reynolds numbers, still in

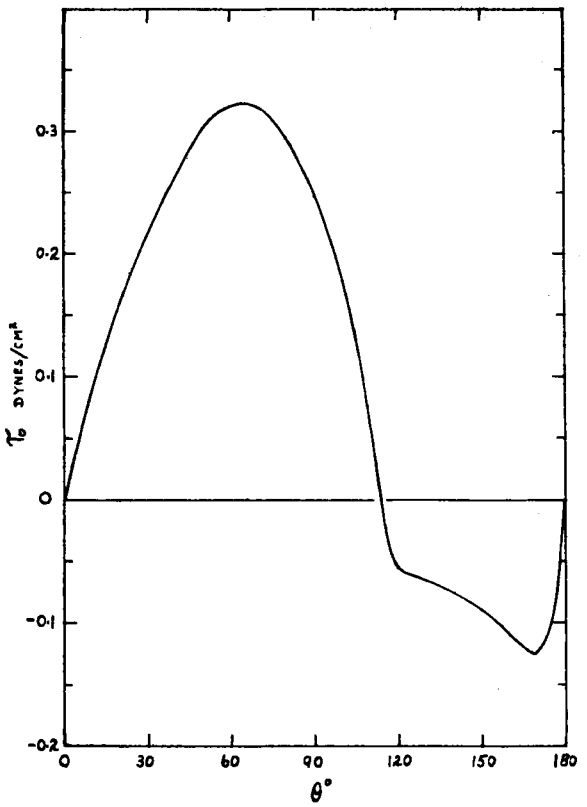

Fig. 17. Intensity of skin friction round sphere $N_{Re} = 200$.

streamline flow conditions, the distributions of mass transfer and skin friction over the surface differ so that the analogy again does not apply. Since conditions around a cylinder are similar to those around a sphere, except that the flow may be treated as two-dimensional instead of three, the same objections to the application of the complete analogy will apply.

Thus for flow around bluff bodies it seems that while the analogy between heat and mass transfer may be applicable, the extension to include momentum transfer is not.

NOTATION

C_D = drag coefficient, dimensionless
C_f = coefficient of total frictional force, dimensionless
D = diameter of sphere
D_v = diffusivity
C_P = specific heat of the fluid
g = gravitational acceleration
h = heat transfer coefficient
k = thermal conductivity
K = mass transfer film coefficient
r = radius of sphere
U_o = undisturbed velocity of flow
U = velocity at the outer edge of the boundary layer
U_{app} = fluid velocity, at sphere position
U_{avg} = average fluid velocity
β = coefficient of cubical expansion
δ = hydrodynamic boundary-layer thickness
θ = angle point of the surface subtended with the forward stagnation point
θ_1 = angle point on surface subtended with the rear stagnation point
μ = absolute viscosity
ν = kinematic viscosity
ρ = density
$\phi(\theta_1) = 1/\sin^2\theta(\frac{1}{2}\theta - \frac{1}{4}\sin 2\theta)$

$N_{Gr} = \dfrac{dD^3\beta\,\Delta T}{\nu^2}$ = Grashof number for heat transfer

$N_{Gr'} = \dfrac{gD^3}{\nu^2}\dfrac{\Delta\rho}{\rho}$ = Grahof number for mass transfer

$N_{Nu} = \dfrac{hD}{k}$ = Nusselt number

$N_{Pr} = \dfrac{C_P\mu}{k}$ = Prandtl number

$N_{Re} = \dfrac{DU_{avg}}{\nu}$ = Reynolds number based on the average velocity

$N_{Re'} = \dfrac{DU_{app}}{\nu}$ = Reynolds number based on the approach velocity

$N_{Sc} = \dfrac{\nu}{D_v}$ = Schmidt number

$N_{Sh} = \dfrac{KD}{D_v}$ = Sherwood number

LITERATURE CITED

1. Axel'rud, G. A., *J. Phys. Chem. (U.S.S.R.)*, **27**, (10), 1446 (1953).
2. Castleman, R. A., *Natl. Advisory Comm. Aeronaut. Tech. Note*, 231 (1925).
3. Colburn, A. P., *Trans. Am. Inst. Chem. Engrs.*, **29**, 174 (1933).
4. Davies, Mansel, and D. M. L. Griffiths, *Trans. Faraday Soc.*, **49**, (12), 1405 (1953).
5. Dryden, C. E., D. A. Strang, and A. E. Withrow, *Chem. Eng. Progr.*, **49**, 191 (1953).
6. Eckert, E. R. G., "Introduction to Heat and Mass Transfer," McGraw-Hill Book Company, Inc., New York (1950).
7. Frossling, N., *Gerl. Beit. zur. Geophysik.*, **52**, 170 (1938).
8. Fuchs, N., *J. Phys. (U.S.S.R.)*, **6**, 224 (1934).
9. Garner, F. H., and R. W. Grafton, *Proc. Roy. Soc. (London)*, (1954), **A224**, 64.
10. Garner, F. H. *Chem. Ind.*, p. 141 (1956).
11. Goldstein, S., "Modern Developments in Fluid Dynamics," Oxford University Press (1938).
12. Grafton, R. W., Ph.D. thesis, Univ. Birmingham, (1953).
13. Hixson, A. W., and S. J. Baum, *Ind. Eng. Chem.*, **34**, 120, (1942).
14. Kramers, H. A., *Physica*, 12, 61 (1946).
15. Keey, R. B., Unpublished work, University of Birmingham (1955).
16. Langmuir, I., *Phys. Rev.* 12, 368 (1918).
17. Linton, W. H., and T. K. Sherwood, *Chem. Eng. Progr.* **46**, 258 (1950).
18. Lohrisch, W., *Forsch. Arb.*, **322**, 1 (1929).
19. McAdams, W. H., "Heat Transmission," 3 ed., McGraw-Hill Book Company, Inc., New York (1951).
20. McNown, J. S., and J. T. Newlin, "Proc. First U. S. National Congress of Appl. Mech." (1951).
21. Merk, H. J., and J. A. Prins, *App. Sci. Res.*, **A4**, 11 (1953).
22. Milikan, C. B., *A.S.M.E. Trans.*, **54**, 2 (1932), *A. P. M.*, 29.
23. Morse, H. W., *Proc. Amer. Acad. Arts. Sci.*, **45**, 363 (1910).
24. Othmer, D. F., and M. S. Thakar, *Ind. Eng. Chem.* **45**, 589 (1953).
25. Powell, R. W., *Trans. Inst. Chem. Engrs.*, **18**, 36 (1940).
26. Ranz, W. E., and W. R. Marshall, *Chem. Eng. Progr.*, **48**, 141 (1952).
27. Sherwood, T. K., *Ind. Eng. Chem.*, **42**, 2077 (1950).
28. ———, and R. L. Pigford, "Absorption and Extraction," 2 ed., McGraw-Hill Book Company, Inc., New York (1952).
29. Stirba, Clifford and D. M. Hurt, *A.I.Ch.E. Journal*, 1 (2), 178 (1955).
30. Tang, Y. S., J. Duncan, and H. E. Schweyer, *Natl. Advisory Comm., Aeronaut. Note* 2867 (1953).
31. Tomotika, S., A.R.C.R. and M. No. 1678 (1936).
32. Ward, A. F. H., and L. H. Brooks, *Trans. Faraday Soc.*, **48**, 1124 (1952).
33. Whitelaw-Gray, R., and H. S. Patterson, "Smoke," Edward Arnold Company, London (1932).
34. Wilke, C. R., *Chem. Eng. Progr.*, **45**, 218 (1949).
35. ———, C. W. Tobias, and Myron Eisenberg, *Chem. Eng. Progr.*, **49**, 663 (1953).

Manuscript submitted February 4, 1957; paper accepted September 12, 1957.